Domain-Specific Interactions of Talin with the Membrane-Proximal Region of the Integrin β3 Subunit†

Tobias S. Ulmer,‡,§ David A. Calderwood,|| Mark H. Ginsberg,*,|| and Iain D. Campbell*,‡

Department of Biochemistry, University of Oxford, South Parks Road, Oxford OX1 3QU, U.K., and Department of Cell Biology, The Scripps Research Institute, 10550 North Torrey Pines Road, La Jolla, California 92037

Received March 7, 2003; Revised Manuscript Received May 5, 2003

ABSTRACT: Activation (affinity regulation) of integrin adhesion receptors controls cell migration and extracellular matrix assembly. Talin connects integrins with actin filaments and influences integrin affinity by binding to the integrins' short cytoplasmic β-tail. The principal β-tail binding site in talin is a FERM domain, comprised of three subdomains (F1, F2, and F3). Previous studies of integrin αIIbβ3 have shown that both F2 and F3 bind the β3 tail, but only F3, or the F2−F3 domain pair, induces activation. Here, talin-induced perturbations of β3 NMR resonances were examined to explore integrin activation mechanisms. F3 and F2−F3, but not F2, distinctly perturbed the membrane-proximal region of the β3 tail. All domains also perturbed more distal regions of the β3 tail that appear to form the major interaction surface, since the β3(Y747A) mutation suppressed those effects. These results suggest that perturbation of the β3 tail membrane-proximal region is associated with talin-mediated integrin activation.

Integrin adhesion receptors mediate cell attachment and are essential for the development and function of multicellular animals (*1*). Integrins are noncovalent $\alpha\beta$ heterodimers of type I transmembrane protein subunits. Each subunit has a large (>700 residue) N-terminal extracellular domain followed by a single membrane-spanning domain that connects it to a generally short (13−70 residue) cytoplasmic tail (*2*, *3*). These tails are involved in the processes that regulate the affinity of the integrin receptor for extracellular ligands (integrin activation) (*1*). Integrin activation thus controls the ability of these receptors to mediate cell adhesion and migration and to remodel the extracellular matrix (*4*). In particular, the membrane-proximal regions of integrin α and β subunits are involved in maintaining integrins in a default low-affinity state (*5*−*7*). Integrin activation also requires membrane-distal integrin β-tail residues (*5*), in particular, a highly conserved NPXY motif (*8*). Thus, integrin activation requires specific amino acids throughout the integrin β cytoplasmic domain.

Structural characterizations of some integrin functional states are available, most notably, the crystal structure of the extracellular part of integrin αvβ3 (*9*), which may represent the low-affinity state based on electron microscopy studies that show global rearrangement of the extracellular integrin domains in different states of activation (*10*). These new data, together with earlier evidence, strongly suggest that the α- and β-tails are in close proximity in the "off" state (reviewed in ref *11*). A number of NMR[1] experiments have been undertaken to observe direct interactions between the tails, but results are, so far, inconsistent. Two studies failed to detect any specific interactions between the αIIb and β3 tails (*12*, *13*), and two studies reported differing interactions between the tails (*14*, *15*).

There is extensive evidence that other intracellular factors, such as the protein talin, are important in integrin activation. Talin fragments are known to bind the β3 tail and to activate integrin αIIbβ3 (*16*, *17*). Talin is an actin binding protein that links integrins to the actin cytoskeleton (*18*) and colocalizes with clustered integrins. Talin is comprised of an N-terminal ∼47 kDa globular head domain (talin-H) and an ∼190 kDa C-terminal rod (talin-R) domain (Figure 1a) (*19*). The head domain contains a FERM domain (*19*) that is the principal integrin binding site (*16*, *20*, *21*) and is involved in integrin activation (*16*, *17*). As in other proteins with FERM domains, e.g., ezrin, radixin, and moesin, some of talin's binding activity is masked in the intact molecule (*21*, *22*). FERM domains have three subdomains, F1, F2, and F3 (*23*). The F3 subdomain appears to be responsible for integrin activation since F3 and F2−F3 (F23), but not F2, can activate integrin αIIbβ3 (*17*).

A recent X-ray crystallographic study of a chimeric construct, containing a fragment of the β3-tail (residues W739−A750) attached to F23, defined some of the key molecular interactions (*23*). These interactions have been confirmed, in the same paper, by NMR studies of interactions between F23 and a separate construct containing an intact

† This work was supported by NIH Grants HL-48728 and HL-31950, the American Heart Association, the Susan G. Komen Breast Cancer Foundation, the Cell Migration Consortium, and the Wellcome Trust.

* Corresponding authors. M.H.G.: tel, +1-858-784-7124; fax, +1-858-784-7343; e-mail, ginsberg@scripps.edu. I.D.C.: tel, +44-1865-275-346; fax, +44-1865-275-253; e-mail, iain.campbell@bioch.ox.ac.uk.

‡ University of Oxford.

§ Present address: Laboratory of Chemical Physics, National Institute of Diabetes and Digestive and Kidney Diseases, National Institutes of Health, Bethesda, MD 20892.

|| The Scripps Research Institute.

[1] Abbreviations: DPC, dodecylphosphocholine; HSQC, heteronuclear single-quantum coherence; K_D, dissociation constant; NMR, nuclear magnetic resonance; SPR, surface plasmon resonance.

10.1021/bi034384s CCC: $25.00
Published on Web 06/10/2003

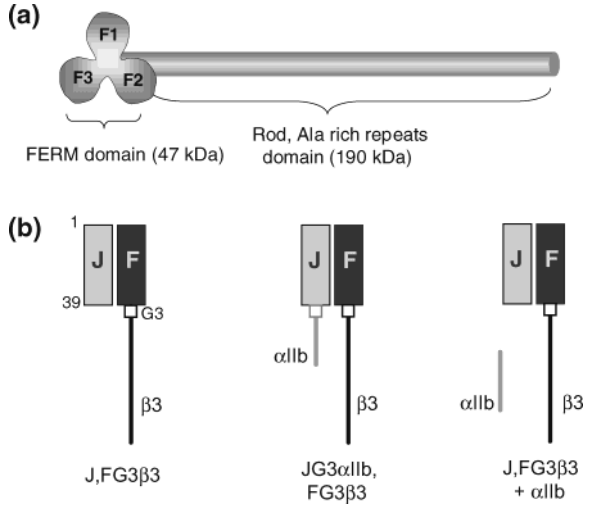

FIGURE 1: (a) Illustration of the domain structure of talin. (b) Illustration of the coiled-coiled construct used to study the integrin αIIbβ3 cytosolic tails. The tails, encompassing integrin αIIb residues K989−E1006 and β3 residues K716−T762, are fused to a heterodimeric coiled coil with subunits termed J and F (residues 1−39) via three glycine linkers, termed G3. A disulfide bond between Cys5 of the J and F subunits ensures proper dimerization of the coiled coil. Only the FG3β3 subunit is ^{15}N labeled in most experiments, and any NMR signals from the J-subunit are thus filtered out. Talin−β3 tail interactions were studied in the complete absence of αIIb, when fused to the J-subunit (JG3αIIb) or with αIIb peptide free in solution.

β3 tail (*23*). These observations are extended here by examining differences in binding of the β3 tail to talin F2, F23, and F3 fragments and by examining effects of the αIIb tail, both free in solution and when brought in close proximity of the β3 tail, within a previously introduced coiled-coil construct (*12*) (Figure 1b). NMR backbone resonance measurements indicate that the activating fragments F3 and F23, but not the F2 subdomain, perturb the membrane-proximal region of the β subunit. All three talin fragments also perturb overlapping, more distal regions of the β3 tail, in agreement with previous mutagenesis studies (*17*). The observed spectral perturbations are suppressed by the β3-(Y747A) mutation. The αIIb tail inhibits the activation of the intact receptor (*24*, *25*). When the αIIb tail was brought into close proximity to the β3 tail, it markedly suppressed F23 perturbation of the membrane-proximal region of the β3 tail, whereas no effects were observed when αIIb peptide was free in solution. These results, using two distinct approaches, suggest that activation of integrins by talin is related to its ability to alter the membrane-proximal region of the β3 tail.

EXPERIMENTAL PROCEDURES

Protein and Peptide Production. Integrin tail model proteins, encompassing integrin αIIb residues K989−E1006 and β3 residues K716−T762, were produced as described previously (*12*). The previous nomenclature (*12*) for the integrin tail model proteins is used here. In brief, an integrin tail is fused to a heterodimeric coiled coil (with subunits termed "J" and "F") via three glycine linkers (termed "G3"; see Figure 1b). A disulfide bond between Cys5 of the J and F subunits ensures proper dimerization of the coiled coil. Free integrin αIIb tail peptide (K989−E1006) was purchased from Alta Bioscience, Birmingham, U.K. Free ^{15}N-labeled αIIb tail peptide was produced as a GST fusion protein in *Escherichia coli* BL21(DE3)pLysS cultured in M9 minimal medium containing 20 mM $^{15}NH_4Cl$. The fusion protein was purified on glutathione−Sepharose beads (Amersham Pharmacia); labeled αIIb tail was removed by thrombin cleavage and further purified on a reverse-phase HPLC column (Vydac). The mass was that expected for the αIIb tail peptide with >98% incorporation of ^{15}N. Talin fragments were produced as described (*16*, *17*). The following nomenclature is used: F2 denotes mouse talin (Swissprot entry P26039) residues S206−L305, F3 denotes mouse talin residues G309−S405 containing a C336S substitution, and F23 denotes chicken talin (*26*) residues E186−Q435. A mouse talin fragment, residues S206−S405, denoted F23M, was also examined for comparison. The C336S substitution in talin F3 did not alter binding to integrin β-tail model proteins in affinity chromatography experiments (data not shown).

NMR Sample Preparation. Freeze-dried integrin tail model proteins were dissolved in the NMR buffer (50 mM phosphate buffer of the desired pH, see below, and 100 mM NaCl) and equilibrated by three ultrafiltration−dilution cycles (1:10 dilution each). Talin fragments were thawed on ice, and the purification buffer was exchanged into the NMR buffer by four ultrafiltration−dilution cycles (1:10 dilution each). Except for F2, protein concentrations were determined by UV spectroscopy using ϵ_{280}(J,FG3β3) = ϵ_{280}(JG3αIIb,-FG3β3) = 10930 M^{-1} cm^{-1}, ϵ_{280}[J,FG3β3(Y747A)] = 9650 M^{-1} cm^{-1}, ϵ_{280}(F3) = 20340 M^{-1} cm^{-1}, and ϵ_{280}(F23) = 23140 M^{-1} cm^{-1}. The concentration of F2 was estimated from SDS−PAGE and 1D ^{1}H NMR spectra. Defined amounts of reagents were combined and concentrated. D_2O (5%) and, if necessary, NMR buffer were added to give a final NMR sample volume of 270 μL. The following samples were prepared at pH 6.1: 0.1 mM J,^{15}N-FG3β3(Y747A) free and with 0.4 mM F2, 0.2 mM F3, and 0.2 mM F23, respectively; 0.1 mM J,^{15}N-FG3β3 free and with 0.4 mM F2, 0.2 mM F3, and 0.2 mM F23, respectively; 0.1 mM ^{15}N-αIIb peptide free and with 0.4 mM F2, 0.2 mM F3, and 0.2 mM F23, respectively. The following samples were prepared at pH 6.6: 0.1 mM JG3αIIb,^{15}N-FG3β3 free and with 0.2 mM F23; 0.1 mM J,^{15}N-FG3β3 free and with 0.2 mM F23. The following sample was prepared at pH 6.8: 0.1 mM J,^{15}N-FG3β3 free and with 0.2 mM F23M. The F23M fragment is less soluble below pH 6.8 than the slightly larger (chicken) F23 fragment. Because pronounced amide solvent exchange at pH 6.8 leads to many unobservable residues at pH 6.8, the F23 fragment was employed for most experiments. Results for F23 and F23M were otherwise indistinguishable within experimental errors (data not shown). The J,FG3β3 samples at pH 6.1 were prepared twice using different protein batches to test reproducibility. After initial NMR data collection free αIIb integrin tail peptide was added to the samples containing J,FG3β3, to final concentrations of 0.8 mM for F2 and 0.4 mM for F3 and F23, respectively.

NMR Spectroscopy. Experiments were performed on spectrometers operating at ^{1}H frequencies of 600 or 750 MHz. Under the conditions used, all talin domains were well folded, as judged from 1D ^{1}H NMR spectra (data not shown). The average amide proton transverse relaxation times (T_2) were estimated by 1-1 echo experiments (*27*) to be ~25 ms for free F2 (11.5 kDa) and F3 (11.1 kDa) and ~11 ms for free F23 (28.9 kDa). The J,FG3β3-bound T_2s were estimated

to be ~19 ms for F2 and F3 and ~9 ms for F23. These figures suggest that the proteins are monomeric at pH 6.1 and 34 °C. ^{1}H−^{15}N HSQC experiments (*28*, *29*) were carried out with acquisition times of 138.1 ms (^{15}N) and 102.4 ms (H^N) at pH 6.1 and 124.3 ms (^{15}N) and 81.9 ms (H^N) at pH 6.6 and 6.8; 25° shifted squared cosine-bell and regular cosine bell window functions were applied. H^N and ^{15}N backbone resonance assignments of the FG3β3 subunit were transferred from 10 mM acetic acid-d_3/acetate-d_3, pH 4.5, 37 °C (*12*), to 50 mM phosphate buffer, pH 6.1−6.8, and 100 mM NaCl, 34 °C, by comparison of the chemical shifts of J,^{15}N-FG3β3 via steps at pH 4.5, 5.5, and 6.5. For the FG3β3(Y747A) subunit it then proved sufficient to compare the H^N and ^{15}N shifts of J,^{15}N-FG3β3(Y747A) in 50 mM phosphate buffer, pH 6.1, and 100 mM NaCl, 34 °C, directly with the shifts in 10 mM acetic acid-d_3/acetate-d_3, pH 4.5, 37 °C. Data were processed and analyzed with Felix 2.3 (Biosym Inc., San Diego, CA).

RESULTS

Effect of Talin Domains on NMR Spectra of the β3 Integrin Tail. Dissociation constants, K_Ds, for the interaction of the β3 tail with F2, F3, and the talin head domain (talin-H), which contains F2−F3 (F23), have been determined by surface plasmon resonance measurements (*17*, *21*). Values of 540 ± 40, 130 ± 10, and 91 ± 4 nM for F2, F3, and talin-H, respectively, suggest that complex formation should be complete under the sample conditions used here. Even though an excess of talin fragment was added in each case, the observed spectra indicate that this was not always the case. Strong perturbations of the NMR resonances of β3 were observed on addition of talin domains. These perturbations can be interpreted as arising in part from chemical exchange between the free and talin-bound states. In the presence of F23, extensive reductions in β3 H−N HSQC signal intensities, accompanied by relatively small H^N and ^{15}N chemical shift changes, were observed with only one signal per β3 residue (Figure 2a), indicating fast exchange. F3 caused extensive reduction in signal intensity for most residues (e.g., A735, A737, K748), but two signals could be detected for some (e.g., I719, F754; Figure 2b), implying that a mixture of slow and fast exchange is obtained in this case. In the presence of F2 most of the β3 residues affected by binding gave rise to two resonances (Figure 2c), indicating that this complex was predominantly in the slow exchange limit.

The β3 Regions Perturbed upon Binding of the Talin Fragments. Comparison of the signal intensities of the β3 resonances in the presence and absence of F23, I/I_0, for each residue, reveals that F23 affects three regions strongly, the membrane-proximal T720−I721 residues, the more distal A735−D740 region, and L746−K748 of the NPLY motif (residues 744−747; Figure 3a). Small effects were also observed for I757−Y759 of the NITY motif, which is somewhat similar in sequence to NPLY. The chemical shift difference between the free and perturbed resonances also follows the I/I_0 pattern (Figure 2a; data not shown). However, in the fast exchange regime, I/I_0 depends both on the square of the chemical shift difference between the free and bound state (ω^2) and the transverse relaxation rate of the bound state (T_{2B}), so it is most sensitive to changes in environment. We note that for a few residues (depicted in Figure 4) no I/I_0 values could reliably be observed, mainly because of signal overlap. The β3(Y747A) mutant inhibits talin binding to β3 tails (*16*) and abolishes the reverse-turn propensity of

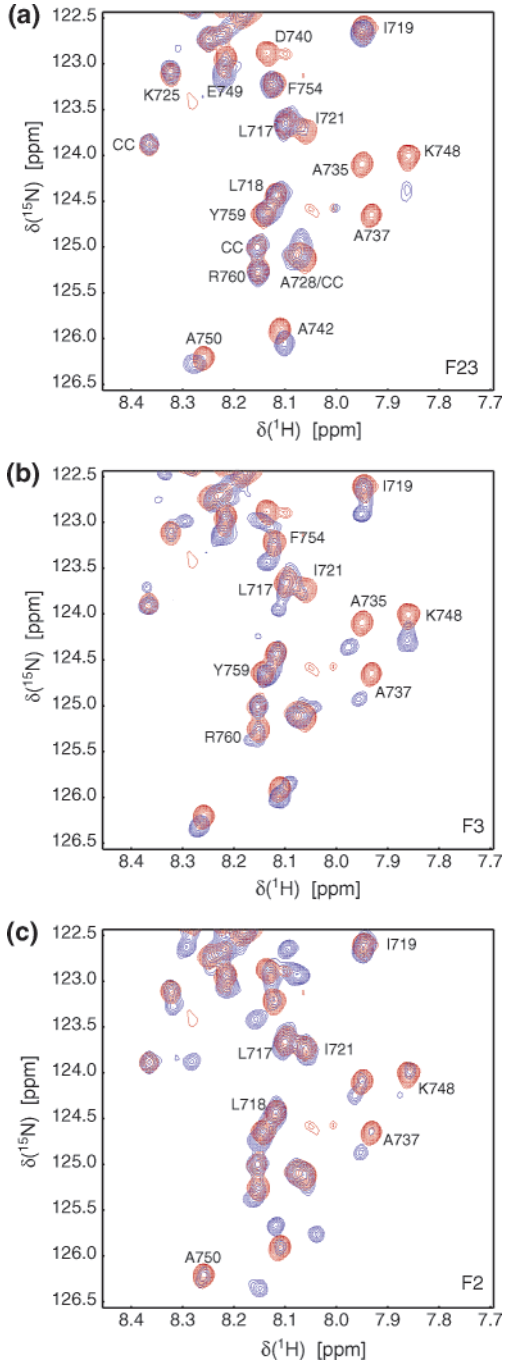

FIGURE 2: Effects of talin F2, F3, and F23 on integrin β3 tail spectra. Superimposed regions of 2D H−N HSQC spectra of the β3 tail alone (red) and in the presence of excess (a) F23, (b) F3, and (c) F2 (blue). The β3 integrin tail is fused to a heterodimeric coiled coil via three glycine linkers. A disulfide bond at the N-terminus of the coiled coil maintains the dimeric state. The properties of β3 within this fusion protein have been described in detail previously (*12*). The β3-bearing coiled-coil subunit, enriched with ^{15}N, is observed exclusively in the HSQC experiments. The free β3 H−N resonances are labeled with their residue numbers; resonances from the coiled coil are labeled as CC. Interactions were studied in 50 mM NaH_2PO_4/Na_2HPO_4 and 100 mM NaCl solutions at pH 6.1, 34 °C, and a ^{1}H frequency of 750 MHz. In the presence of F23 extensive broadening of β3 resonances was observed, but only one signal per residue was found. For F3 some residues exhibit two resonances in the presence of excess F3, and with F2 most residues appear to exhibit two signals in the presence of excess F2.

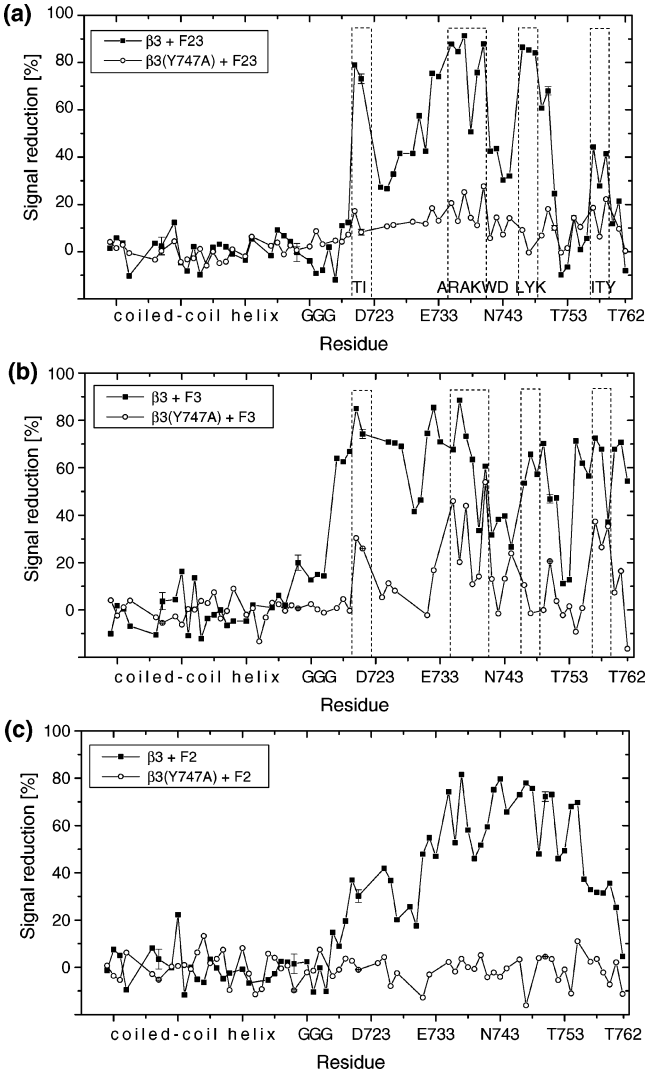

FIGURE 3: Effects of talin F2, F3, and F23 binding on integrin β3 signal intensities. The H−N HSQC signal intensities of free, *I*, and bound, I_0, β3 resonances are quantified for each residue for (a) F23, (b) F3, and (c) F2. The I/I_0 ratio is depicted as reduction in signal intensity. Both the wild-type β3 tail and its β3(Y747A) mutant were examined. In contrast to the β3 tail, no significant changes were observed for the coiled-coil resonances. To correct for uniform variations in peak intensity, caused by changes in conditions such as shimming or viscosity, the average intensity of the coiled-coil resonances, which ranged from 0.78 to 1.03 throughout all experiments, was set to unity in each case, and the other peaks were proportionately scaled. For clarity error bars are omitted for most residues; residues with errors larger than 10% are not shown. Gaps also arise because of other factors, such as spectral overlap and a proline at position 745.

NPLY present in the β3 tail (*12*). Here, it suppressed the majority of the observed intensity changes, with no broadening remaining for L746−K748 and only very weak broadening evident for T720−I721 and A735−D740 (Figure 3a).

In the presence of F3, with β3 residues in both the slow and fast exchange limit, the signal at the position of the "free" resonance was used to calculate the I/I_0 ratio for residues that exhibited both the free and bound signal. The extracted I/I_0 pattern shows that large effects are obtained for most β residues (Figure 3b). For the more membrane-proximal residues this seems to be due to slow exchange kinetics of these residues (e.g., L717, I719; Figure 2b). For residues close to the C-terminus, both slow and fast exchange was

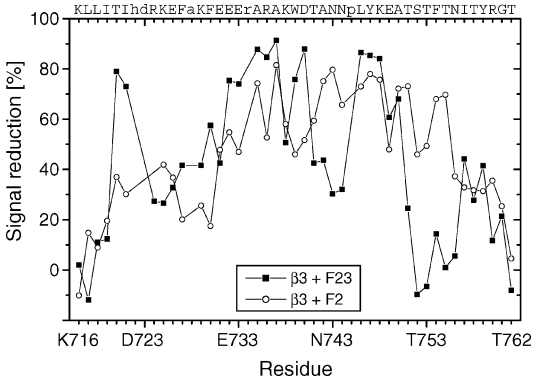

FIGURE 4: Comparison of β3 resonance perturbation obtained on addition of F23 and F2. In contrast to F2, the membrane-proximal T720−I721 residues are perturbed by F23. The membrane-proximal region is defined here as K716−K725. The whole β3 sequence is shown; lower case letters indicate residues for which no I/I_0 values could be obtained using F23.

observed (e.g., Y759, R760; Figure 2b). Thus, the F3−β3 interaction appears to be in an unfavorable exchange regime, which makes the F3−β3 spectrum relatively difficult to interpret. Addition of F3 to β3(Y747A) produced much less broadening than observed on addition of F3 to β3 (Figure 3b), consistent with reduced binding to the β3(Y747A) mutant (*17*). The corresponding HSQC spectrum exhibited only fast exchange characteristics (data not shown); under these conditions, the remaining broadening pattern for β3-(Y747A) residues corresponds to that obtained for the β3−F23 interaction, except L746−K748 (Figure 3a,b), suggesting that the two activating talin fragments, F3 and F23, interact with essentially the same regions of the β3 tail.

In the presence of F2, most residues are in the slow exchange limit, and the I/I_0 pattern is again simpler than for F3 (Figure 3c). Residues encompassing A735−T755 are involved in interactions, whereas membrane-proximal residues do not appear to be substantially involved (e.g., L717, L718, I719, I721; Figures 2c and 3c). Although large reductions in signal intensity of the free signal are observed in the presence of excess F2 (up to about 80%; Figure 3c), the free state is still populated. In this case, with predominantly slow exchange, information could also be obtained by comparing the chemical shifts between the free and bound states, but the assignments of the bound state were not available for peaks with large shifts (Figure 2c). For the β3-(Y747A) interaction with F2, there is essentially no visible reduction in peak intensity compared to the free state (Figure 3c). Taken together, these results show that F2 binding to the β3 tail depends on both the NPLY motif and additional residues in the A735−T755 region. The nonactivating F2 fragment exhibited a much weaker interaction with the membrane-proximal residues than F23 or F3 as depicted in Figure 4. Therefore, while all three talin fragments interact with membrane-distal β3 tail residues, in particular the NPLY motif, only the activating F3 and F23 fragments perturb the membrane-proximal T720−I721 residues.

Influence of α*IIb on the* β*3−Talin Interaction.* Integrin α subunit cytoplasmic tails contribute to regulation of the integrin activation state (*5*, *24*). We therefore examined the effects of αIIb on the activating β3−F23 interaction. Free αIIb tail peptide was found to have no effect on the interaction, within experimental error (Figure 5a). Addition

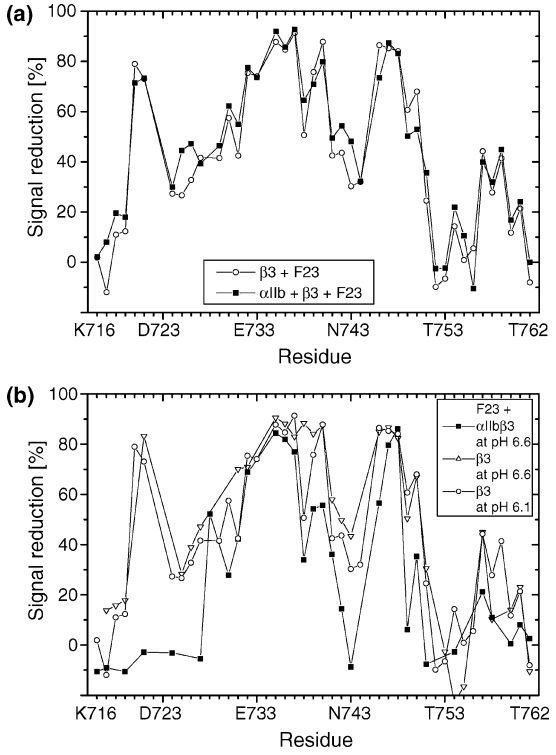

FIGURE 5: Influence of the αIIb tail on the interaction of the integrin β3 tail with F23. (a) The F23−β3 perturbations, observed in the absence of the αIIb tail, are compared with those observed with excess free αIIb tail peptide. The results are indistinguishable within experimental errors. (b) The F23−β3 perturbations, observed in the absence of the αIIb tail, are compared with those observed when both tails are fused to a two-helix coiled-coil construct. For solubility reasons the coiled-coil construct, with both αIIb and β3 tails attached, was studied at the slightly higher pH of 6.6 compared to pH 6.1 when only β3 is attached. Compared to pH 6.1, amide exchange with solvent water at pH 6.6 is, on average, about 3.2 times faster. This rapid exchange rate limits the observation of many resonances and leads to more missing data points. The pH 6.6 results for the coiled-coil construct do, however, confirm the protection effect of αIIb on β3 resonance intensity reductions.

of F23, or any of the other talin fragments, to the free αIIb tail also induced no observable H−N chemical shift or signal intensity changes (data not shown), in agreement with affinity chromatography studies which did not detect any binding to αIIb (*17*). The β3 tail studied here is fused C-terminally to one of the helices of the coiled-coil construct. The αIIb tail can thus be placed parallel to β3 in a heterodimeric construct (Figure 1b). As shown in Figure 5, the αIIb tail then prevents F23-induced broadening of the membrane-proximal β3 residues (T720−I721). The presence of the αIIb tail thus can protect the membrane-proximal region of the β3 tail from interaction with talin.

DISCUSSION

We have identified talin binding regions in the β3 tail by monitoring selective changes of NMR resonances, in the presence of different talin subdomains: F2, F3, and F2−F3 (F23). For F23 and F3 spectral changes were observed in three main regions (T720−I721, A735−D740, and L746−K748). In contrast, F2 binding to the β3 tail depends mainly on residues in the A735−T755 region, especially residues 744−747 (NPLY). The most obvious explanation for these observations is direct talin binding to these β3 tail regions. A less likely explanation for some of the observed changes is that binding to some regions (e.g., to NPLY) indirectly changes the resonances in the membrane-proximal region by structuring the β3 tail. There is substantial independent evidence for direct interactions. Patil and co-workers have reported that talin interacts directly with peptides from the membrane-proximal region (*20*). In the current study, introduction of the αIIb tail in a heterodimeric construct markedly suppresses perturbation of the membrane-proximal region of β3 by F23. The more membrane-distal sequences of the β3 tail that are affected, particularly in the vicinity of the NPLY sequence, are strongly implicated in direct interactions by the binding of peptides derived from β3 (*30*) or β1A (*18*). The effects of mutations in this region on talin binding (*30*, *31*) have also been verified directly here by the observation of minimal spectral changes with the β3(Y747A) mutant. Chemical shift perturbations of β3 were also reported to be pronounced for residues I719−H722 in the presence of the talin head domain (*14*).

Both F2 and F3 domains of the F23 fragment have the capacity to bind the β3 tail; however, in cases where the F3 domain is present, and available, it is likely to be responsible for interactions of the entire head domain with β3 because of its higher intrinsic affinity. However, the high-affinity integrin binding site in the talin head domain is masked in intact talin (*21*), and the affinity of intact talin is similar to that of F2 (*17*, *21*). This raises the possibility that, in full-length talin, the F3 domain may be masked; talin could then interact with integrins via its F2 domain, permitting tethering of inactive integrins to the actin cytoskeleton.

The central finding of the current study is that spectral perturbations of the membrane-proximal region (K716−K725) of the β3 subunit are correlated with the capacity of talin fragments to activate integrin αIIbβ3. Thus, the activating F3 and F23 talin fragments perturb this region in a characteristic fashion, whereas effects for the nonactivating F2 fragment are minor. As mutational perturbations of the membrane-proximal portion of the αIIb or β3 integrin cytoplasmic domains lead to integrin activation (*5*−*7*, *24*, *32*), the capacity of talin to activate integrins is likely to be related to its ability to alter the membrane-proximal region of β3. In this context we also note that the presence of the αIIb tail in a heterodimeric construct protects the membrane-proximal region of the β3 tail from interaction with talin. However, the biological significance of this observation and the underlying mechanism remain unclear.

How could talin binding to this membrane-proximal region of the β3 tail lead to integrin activation? Mutational studies (*6*), experiments with engineered tails (*33*), and a recent NMR study (*14*) suggest that membrane-proximal αIIb−β3 contacts contribute to the maintenance of integrin αIIbβ3 in the inactive state. Vinogradova et al. proposed that the αIIb tail and talin compete for interactions with the membrane-proximal region of the β3 tail with the dissociation of the αIIb and β3 tails offering an integrin activation mechanism (*14*). The data presented here, which suggest that a membrane-proximal region of β3 can interact with the talin F3 domain when the αIIb tail is absent from the coiled-coil construct support this idea. Glycosylation mapping studies (*34*) suggest that the membrane-proximal region may, at times, be embedded in the membrane. An alternative activation mechanism, therefore, is that talin binding to membrane-proximal

residues of β3 could change the border of the integrin transmembrane and cytoplasmic domain. Further support for this model was recently provided by an NMR study of the transmembrane and cytosolic portion of the β3 tail in DPC micelles (*35*). Another recent study by the same group suggests that subsequent oligomerization of the membrane-spanning regions may contribute to integrin activation (*36*). Yet another study applied molecular dynamics simulations and predicted that interactions between the membrane spanning regions would be important (*37*). Additional studies will be needed to evaluate the role of each of these mechanisms in the integrin activation process.

REFERENCES

1. Schwartz, M. A., Schaller, M. D., and Ginsberg, M. H. (1995) *Annu. Rev. Cell Dev. Biol. 11*, 549−599.
2. Arnaout, M. A., Goodman, S. L., and Xiong, J. P. (2002) *Curr. Opin. Cell Biol. 14*, 641−651.
3. Shimaoka, M., Takagi, J., and Springer, T. A. (2002) *Annu. Rev. Biophys. Biomol. Struct. 31*, 485−516.
4. Woodside, D. G., Liu, S., and Ginsberg, M. H. (2001) *Thromb. Haemostasis 86*, 316−323.
5. O'Toole, T. E., Katagiri, Y., Faull, R. J., Peter, K., Tamura, R., Quaranta, V., Loftus, J. C., Shattil, S. J., and Ginsberg, M. H. (1994) *J. Cell Biol. 124*, 1047−1059.
6. Hughes, P. E., DiazGonzalez, F., Leong, L., Wu, C. Y., McDonald, J. A., Shattil, S. J., and Ginsberg, M. H. (1996) *J. Biol. Chem. 271*, 6571−6574.
7. Rabb, H., Michishita, M., Sharma, C. P., Brown, D., and Arnaout, M. A. (1993) *J. Immunol. 151*, 990−1002.
8. O'Toole, T. E., Ylanne, J., and Culley, B. M. (1995) *J. Biol. Chem. 270*, 8553−8558.
9. Xiong, J. P., Stehle, T., Diefenbach, B., Zhang, R. G., Dunker, R., Scott, D. L., Joachimiak, A., Goodman, S. L., and Arnaout, M. A. (2001) *Science 294*, 339−345.
10. Takagi, J., Petre, B. M., Walz, T., and Springer, T. A. (2002) *Cell 110*, 599−611.
11. Hynes, R. O. (2002) *Cell 110*, 673−687.
12. Ulmer, T. S., Yaspan, B., Ginsberg, M. H., and Campbell, I. D. (2001) *Biochemistry 40*, 7498−7508.
13. Li, R. H., Babu, C. R., Lear, J. D., Wand, A. J., Bennett, J. S., and DeGrado, W. F. (2001) *Proc. Natl. Acad. Sci. U.S.A. 98*, 12462−12467.
14. Vinogradova, O., Velyvis, A., Velyviene, A., Hu, B., Haas, T. A., Plow, E. F., and Qin, J. (2002) *Cell 110*, 587−597.
15. Weljie, A. M., Hwang, P. M., and Vogel, H. J. (2002) *Proc. Natl. Acad. Sci. U.S.A. 99*, 5878−5883.
16. Calderwood, D. A., Zent, R., Grant, R., Rees, D. J. G., Hynes, R. O., and Ginsberg, M. H. (1999) *J. Biol. Chem. 274*, 28071−28074.
17. Calderwood, D. A., Yan, B., de Pereda, J. M., Alvarez, B. G., Y., F., Liddington, R. C., and Ginsberg, M. H. (2002) *J. Biol. Chem. 277*, 21749.
18. Horwitz, A., Duggan, K., Buck, C., Beckerle, M. C., and Burridge, K. (1986) *Nature 320*, 531−533.
19. Rees, D. J. G., Ades, S. E., Singer, S. J., and Hynes, R. O. (1990) *Nature 347*, 685−689.
20. Patil, S., Jedsadayanmata, A., Wencel-Drake, J. D., Wang, W., Knezevic, I., and Lam, S. C. T. (1999) *J. Biol. Chem. 274*, 28575−28583.
21. Yan, B., Calderwood, D. A., Yaspan, B., and Ginsberg, M. H. (2001) *J. Biol. Chem. 276*, 28164−28170.
22. Martel, V., Racaud-Sultan, C., Dupe, S., Marie, C., Paulhe, F., Galmiche, A., Block, M. R., and Albiges-Rizo, C. (2001) *J. Biol. Chem. 276*, 21217−21227.
23. Garcia-Alvarez, B., de Pereda, J. M., Calderwood, D. A., Ulmer, T. S., Critchley, D., Campbell, I. D., Ginsberg, M. H., and Liddington, R. C. (2003) *Mol. Cell 11*, 49−58.
24. O'Toole, T. E., Mandelman, D., Forsyth, J., Shattil, S. J., Plow, E. F., and Ginsberg, M. H. (1991) *Science 254*, 845−847.
25. Vinogradova, O., Haas, T., Plow, E. F., and Qin, J. (2000) *Proc. Natl. Acad. Sci. U.S.A. 97*, 1450−1455.
26. Hemmings, L., Rees, D. J. G., Ohanian, V., Bolton, S. J., Gilmore, A. P., Patel, B., Priddle, H., Trevithick, J. E., Hynes, R. O., and Critchley, D. R. (1996) *J. Cell Sci. 109*, 2715−2726.
27. Sklenar, V., and Bax, A. (1987) *J. Magn. Reson. 74*, 469−479.
28. Boyd, J., Soffe, N., John, B., Plant, D., and Hurd, R. (1992) *J. Magn. Reson. 98*, 660−664.
29. Grzesiek, S., and Bax, A. (1993) *J. Am. Chem. Soc. 115*, 12593−12594.
30. Kaapa, A., Peter, K., and Ylanne, J. (1999) *Exp. Cell Res. 250*, 524−534.
31. Pfaff, M., Liu, S. C., Erle, D. J., and Ginsberg, M. H. (1998) *J. Biol. Chem. 273*, 6104−6109.
32. Crowe, D. T., Chiu, H., Fong, S., and Weissman, I. L. (1994) *J. Biol. Chem. 269*, 14411−14418.
33. Lu, C. F., Takagi, J., and Springer, T. A. (2001) *J. Biol. Chem. 276*, 14642−14648.
34. Armulik, A., Nilsson, I., von Heijne, G., and Johansson, S. (1999) *J. Biol. Chem. 274*, 37030−37034.
35. Li, R. H., Babu, C. R., Valentine, K., Lear, J. D., Wand, A. J., Bennett, J. S., and DeGrado, W. F. (2002) *Biochemistry 41*, 15618−15624.
36. Li, R., Mitra, N., Gratkowski, H., Vilaire, G., Litvinov, R., Nagasami, C., Weisel, J. W., Lear, J. D., DeGrado, W. F., and Bennett, J. S. (2003) *Science 300*, 795−798.
37. Gottschalk, K. E., Adams, P. D., Brünger, A. T., and Kessler, H. (2003) *Protein Sci. 11*, 1800−1812.

BI034384S